Published in final edited form as:
J Am Chem Soc. 2009 October 14; 131(40): 14345–14354. doi:10.1021/ja903773f.

Crystal Structures of Penicillin-Binding Protein 6 from *Escherichia coli*

Yu Chen[†], **Weilie Zhang**[‡], **Qicun Shi**[‡], **Dusan Hesek**[‡], **Mijoon Lee**[‡], **Shahriar Mobashery**[‡], and **Brian K. Shoichet**[†]

Shahriar Mobashery: mobashery@nd.edu; Brian K. Shoichet: shoichet@cgl.ucsf.edu

[†]Department of Pharmaceutical Chemistry, University of California San Francisco, Byers Hall, Room 508D, 1700 Fourth Street, San Francisco, California 94158-2550

[‡]Department of Chemistry and Biochemistry, 423 Nieuwland Science Center, UniVersity of Notre Dame, Notre Dame, Indiana 46556

Abstract

Penicillin-binding protein 6 (PBP6) is one of the two main DD-carboxypeptidases in *Escherichia coli*, which are implicated in maturation of bacterial cell wall and formation of cell shape. Here, we report the first X-ray crystal structures of PBP6, capturing its apo state (2.1 Å), an acyl-enzyme intermediate with the antibiotic ampicillin (1.8 Å), and for the first time for a PBP, a preacylation complex (a "Michaelis complex", determined at 1.8 Å) with a peptidoglycan substrate fragment containing the full pentapeptide, NAM-(L-Ala-D-isoGlu-L-Lys-D-Ala-D-Ala). These structures illuminate the molecular interactions essential for ligand recognition and catalysis by DD-carboxypeptidases, and suggest a coupling of conformational flexibility of active site loops to the reaction coordinate. The substrate fragment complex structure, in particular, provides templates for models of cell wall recognition by PBPs, as well as substantiating evidence for the molecular mimicry by β-lactam antibiotics of the peptidoglycan acyl-D-Ala-D-Ala moiety.

Introduction

The bacterial cell wall, also referred to as the cross-linked peptidoglycan, is constructed of a repeating disaccharide unit of *N*-acetylglucosamine (NAG) and *N*-acetylmuramic acid (NAM), with NAM bearing a peptide moiety.[1,2] Cell wall polymerization includes two enzymatic reactions, a transgly-cosylation that links the disaccharides to form the glycan backbone and a transpeptidation that cross-links the peptides, creating a mesh-like structure. The synthesis and remodeling of bacterial cell wall is performed mainly by penicillin-binding proteins (PBPs), which are classified into high-molecular mass (HMM) and low-molecular mass (LMM) subgroups.[3,4] As suggested by their name, these PBPs are the primary targets of the β-lactam antibiotics. They and related β-lactam recognition enzymes, such as β-lactamases, have been the focus of intense mechanistic, structural, and medicinal chemistry research.[4–12] DD-Carboxypeptidases are members of LMM PBPs that cleave the peptide bond between the two terminal D-alanines of the muramyl peptide, an alteration in the peptidoglycan structure that moderates the degree of cross-linking of the cell wall, a function performed by transpeptidases.[13]

There are two primary DD-carboxypeptidases in *Escherichia coli*, PBP5 and PBP6,[14] which together account for 85% of the copy numbers of all PBPs.[15] Like other PBPs, they contain

Correspondence to: Shahriar Mobashery, mobashery@nd.edu; Brian K. Shoichet, shoichet@cgl.ucsf.edu.

active site sequence motifs essential for catalysis, including Ser-X-X-Lys, Ser-X-Asn and Lys-Thr-Gly, which are also largely shared with serine-based β-lactamases, such as TEM-1 and AmpC.[16] The acylation half-reaction, common to all these enzymes, involves the nucleophilic attack by serine at the carbonyl carbon of the penultimate D-Ala residue in the peptidoglycan, which results in a tetrahedral high-energy intermediate. The collapse of this species gives rise to an acylenzyme intermediate. In the second half-reaction for DD-carboxypeptidases like PBP6, a water molecule attacks this acylenzyme to generate another tetrahedral high-energy species, which in turn collapses to regenerate the catalyst and release a peptidoglycan shortened by one amino acid.

The reaction catalyzed by DD-carboxypeptidases has been investigated mostly using PBP5 as a model system.[17–21] In addition to the nucleophilic serine (Ser44 in PBP5), several active site residues have been implicated in the catalytic mechanism, particularly the lysine in the Ser-X-X-Lys motif (Lys47 in PBP5), which constitutes the catalytic Ser-Lys diad. Recent QM/MM calculations indicate that Lys47 acts as the general base for both the acylation and deacylation steps of the reaction.[17] A boronic acid transition state analog crystal structure also suggests that Ser110 in the Ser-X-Asn motif may contribute to the activation of the nucleophilic water in its attack on the acyl-enzyme complex. Additionally, studies on PBP5 G105D mutant have implicated another region in catalysis, the loop formed by residues 74–90.[19,22] Residues from this region have extensive contacts with the Ser-X-Asn motif. Deletion of this loop abolished the carboxypeptidase activity.[19] The G105D mutation that had similar effects on the enzyme activity also caused disordering of this loop region.[19,22]

In contrast to PBP5, there have been few studies on PBP6 and the biological roles of these DD-carboxypeptidases remain uncertain.[13] DD-Carboxypeptidases are not critical for bacterial growth in cultured media, but their functions are necessary for the health of the organism, especially for maintaining normal cell morphology.[23–25] More broadly, and despite the close attention that PBPs and β-lactam-recognizing proteins have long received, there remain unexpected gaps in our understanding of these enzymes. Perhaps most prominent among these is the lack of structures of a sizable peptidoglycan substrate bound to any PBP. Fragments containing part of the substrate peptide and in complex with deactivated enzymes were used to shed light on the enzymatic reaction catalyzed by PBPs.[26] Since the substrate is a polymer, larger substrates would more fully illuminate the recognition event and the reaction mechanisms of PBPs. Furthermore, these complexes would be useful in understanding how β-lactam compounds mimic these substrates to afford inhibition of PBPs.[27]

Here we investigate by X-ray crystallography both the specifics of PBP6 structure and function, and general questions of substrate and inhibitor recognition in this family of enzymes. We present the first X-ray structures of PBP6 from *E. coli*, whose apo enzyme structure we determine at 2.1 Å. The synthesis of a key peptidoglycan fragment containing the *N*-acetyl-muramyl (NAM) moiety bearing the complete pentapeptide unit (L-Ala-D-isoGlu-L-Lys-D-Ala-D-Ala), allow us to explore a complex between the wild-type PBP6 and a full muramyl peptide substrate, for the first time. We determined the X-ray structure of the preacylation complex (“Michaelis complex”) with this substrate fragment and an acyl-enzyme complex with the antibiotic ampicillin to 1.8 Å. Together with earlier DD-carboxypeptidase structures, these three structures enable a detailed structural analysis of the reaction coordinates of these LMM PBPs, and speak to longstanding questions of the correspondence between β-lactams and the peptidoglycan substrates they are thought to mimic.

Materials and Methods

Cloning of the dacC Gene for Expression of PBP6 in the Cytoplasm

To express PBP6 in the cytoplasm lacking the signal peptide and the anchor, the *dacC* gene was PCR-amplified from the chromosome of *E. coli* K12 using two custom-synthesized primers EcPBP6Nde: 5′-CAT*CATATG*ACGCAATACTCCTCTCTC-CTTCGTGGT-3′ and PBP6EcR 5′-GTA*AAGCTT*AAGAGAAC-CAGCTGCCGAACCACTGA-3′. These primers included the recognition sequences for restriction endonucleases *NdeI* and *HindIII* (italicized in the primer). The PCR product was purified by electrophoresis, digested by *NdeI* and *HindIII* and cloned into the corresponding sites of pET24a(+) (Novagen). The truncated protein contains residues 28–378 of the full-length PBP6, in addition to a new N-terminal methionine.

Expression and Purification of PBP6

For expression of PBP6, *E. coli* BL21(DE3) cells were transformed with the pET24a(+)-based construct containing the *dacC* gene. Colonies containing the construct were selected on LB agar supplemented with 30 μg/mL of kanamycin. Selected cells were incubated overnight in 5 mL of LB medium supplemented with 30 μg/mL of kanamycin. Cells were diluted into 500 mL of fresh kanamycin-supplemented (30 μg/mL) LB medium and growth was continued with agitation (120 rpm) at 37 °C until the culture reached an $OD_{60}0$ of 0.8. Isopropyl-β-D-thiogalactoside (IPTG) was added at this stage to a concentration of 0.4 mM and the culture was incubated at 20 °C for an additional 12 h. All subsequent steps were performed at 4 °C. Cells were harvested by centrifugation, resuspended in 50 mM NaHCO3, 0.15 M NaCl, 0.1% Triton X-100, pH 9.5 and were disrupted by 30 sonication cycles (30 s of burst and 30 s of rest for each cycle). Bacterial debris was removed by centrifugation at 21 000*g* for 40 min. The supernatant was mixed with 3.5 g CH Sepharose 4B (Pharmacia Biotech) coupled with 600 mg ampicillin.[18] The protein-binding step was performed on an orbital shaker at room temperature for 30 min. The resin was transferred onto a sintered glass filter and was washed with 1 L of 20 mM Tris, 1 M NaCl, 0.1% Triton X-100, pH 9.0 for 15 min. PBP6 was eluted using 0.5 M Tris, 1 M NH2OH, pH 9.0. The elution buffer was added directly to the resin on the sintered glass filter. Resin was gently stirred for 15 min and then separated from the liquid phase by filtration. The filtrate containing PBP6 was dialyzed against 25 mM NaHCO3, 0.15 M NaCl, 0.1% Triton X-100, pH 9.5. The protein was subsequently concentrated in an Ultrafree-15 Centrifugal Filter Device (Millipore). The concentration of the protein was determined spectrophotometrically using the BCA Protein Detection Kit (Pierce). SDS-PAGE showed that the purity of PBP6 was more than 98%.

Crystallization and Structure Determination

PBP6 (12 mg/ mL, in 25 mM NaHCO3, 0.15 M NaCl, 0.1% Triton X-100, pH 9.5) was crystallized in 30% PEG 8000, 0.1 M acetate, and 0.2 M Li_2SO_4, pH 4.5, from hanging drops at 19 °C. Final concentration of protein in the mixed drop was 6 mg/mL. The final pH in the drop was approximately 4.5, as indicated by litmus paper check of the drop and the pH meter reading of larger volumes of the same mixed buffer. Crystals appeared after 4–5 days, with one dimension elongated (100 × 100 × 300 to 50 × 50 × 500 μm). Crystals were flash frozen in liquid nitrogen directly or first transferred to a stabilization solution containing 20% PEG 8000, 0.06 M acetate, 0.1 M Li_2SO_4 and 10% sucrose, pH 4.5. For the determination of complex structures, crystals were transferred to the same stabilization solution containing 25 mM ligand (substrate fragment or ampicillin, see Figure 1) and were flash frozen after being soaked for 3 h. Diffraction was measured at Beamline 8.3.1 of the Advanced Light Source (ALS), Berkeley, California and processed with HKL2000.[28] Molecular replacement was carried out using Phaser[29] and a homology model from Modbase that was calculated by Modeler from the apo PBP5 structure (1NZO).[30,31] Initial

attempts to use the whole homology model as the search structure failed to return meaningful results. The two domains of the model were subsequently used as separate entities in the search. Four copies of the larger *N*-terminal domains and three copies of the smaller *C*-terminal domains were identified in the molecular replacement result. This partial model and a fourth *C*-terminal domain was used as the input for another molecular replacement. The result produced the complete tetramer in the asymmetric unit. Refinement and model rebuilding were carried out in CCP4 and coot.[32,33] For the complex structures with the substrate fragment and ampicillin, the ligand was modeled after a few rounds of refinement on the protein chains and water molecules. The Fo-Fc density for the ligand was unambiguous at this stage. The starting coordinates for the ligand was taken from those of the same or a similar ligand in previously determined structures (PDB 2EAX for the substrate fragment[34] and 2EX6 for ampicillin[35]). Both ligands were refined with full occupancy.

Data Deposition

The structures have been deposited in the Protein Data Bank with accession codes 3IT9, 3ITA, and 3ITB.

Results

The gene for PBP6, except the sequence for the signal peptide and the membrane anchor, was cloned for expression in the cytoplasm of *E. coli*. The soluble protein was purified in a single affinity chromatographic step. The protein was crystallized at pH 4.5 in the $P2_1$ space group. A substrate fragment—the *N*-acetylmuramic pentapeptide ("muramyl peptide")—and ampicillin were soaked into the crystals to obtain the complex structures (Figure 1). The apo structure was determined by X-ray crystallography to 2.1 Å resolution, while both of the complex structures were determined to 1.8 Å (Table 1). There are four monomers in each asymmetric unit (Figure 2a). For both complex structures, there is only one well-defined ligand in the asymmetric unit, interacting with the active site of monomer 3 for the preacylation complex and that of monomer 1 for the acyl-enzyme complex. Although model refinement was affected by the disorder of some loops and the relatively low data/ parameter ratio, due to the large number of atoms in each asymmetric unit (Table 1), the majority of the protein and ligand residues are well ordered and the electron density for the ligand is unambiguous in each case.

Overall Structure

The four monomers in each asymmetric unit share nearly identical backbone conformations in most parts of the protein except for certain loops, including those at the active site, a subject to which we will return. For the apo structure, the pairwise rmsd values between the Cα traces of two monomers (343 atoms aligned) range from 0.37 to 0.66 Å. The overall monomer structure resembles that of PBP5, with an rmsd of 1.04 Å between the CR atoms of PBP5 and monomer 1 of PBP6 (342 atoms aligned) (Figure 2b).[19] As in PBP5, each monomer is organized in two domains, a large *N*-terminal domain and a smaller β-sheet rich *C*-terminal domain. The angles between the two domains vary slightly among the four monomers. The active site of the protein resides in the *N*-terminal domain. Both the active site configuration and the topography of this domain resemble those of class A β-lactamases.[12,36,37]

The tetramer in each asymmetric unit is organized as a dimer of dimers loosely associated with one another (Figure 2a). Each dimer enjoys some degree of symmetry, although there are substantial differences between the two monomers in terms of the contributing residues and their specific interactions at the dimer interface. The dimer interface is also different

between the two dimers in the asymmetric unit. It is uncertain whether the crystallographic dimer interface is relevant in the membrane-anchored form of the enzyme, though the protein appears to behave as a monomer in solution, based on the behavior of purified protein in a nondenaturing gel. As discussed below, the presence of the crystallographic dimer does affect the contacts made by the large muramyl peptide.

Apo Active Site

The apo PBP6 active site resembles that of PBP5 (Figure 3).[19] Most active site residues adopt the same conformations among all four monomers, including the nucleophilic Ser40 and the general base Lys43 in the Ser-X-X-Lys motif, Ser106 and Asn108 from the Ser-X-Asn sequence, Lys209 and Thr210 from the Lys-Thr-Gly triad. Lys43 forms three hydrogen bonds with Ser40Oγ (2.7 Å), Asn108Oδ1 (2.7 Å) and the backbone carbonyl oxygen of His147 (3.0 Å). Given the acidic pH at which this complex was crystallized, Lys43 is likely charged and thus acts as a donor in all three hydrogen bonds, though it may well be in the free-base form during catalysis at higher pH values, where it would accept a hydrogen bond from the catalytic Ser40.[17,18] Lys209 hydrogen bonds with Ser106Oγ (2.9 Å) as well as the backbone carbonyl of Val102 (3.0 Å) and Ile103 (2.8 Å). Lys209 is likely to be positively charged in PBP6 and function as donor in all three hydrogen bonds. The corresponding lysine in PBP5, Lys213, is known to be protonated from titration studies on that enzyme.[18] The corresponding Lys234 from class A β-lactamases has also been shown to be charged in ultrahigh resolution X-ray structures.[38,39]

The presence of sulfate molecules, from the crystallization buffer, in the active site of the apo enzyme mimics interactions that will be defined for the substrate and ampicillin complexes in this report (Figure 3c). The sulfate hydrogen bonds with Arg194, Thr210, Arg244 and Thr212, and via an ordered water molecule with Ser106. In monomer 2, the sulfate molecule also hydrogen bonds with Arg190 from monomer 1 (Figure 3c) The conformations of Arg244 and Thr210 remain largely unchanged in all four monomers. These conformations are similar to those observed in the complex structure of PBP5 and a peptidemimetic cephalosphorin, and are different from those in the apo PBP5 protein.[19,21] The binding of the ligand in PBP5 active site induces conformational changes in residues 242–248, bringing the Arg244 counterpart (Arg248) closer to the car-boxylate group on the ligand. In PBP6, Arg244 appears to be coordinated by more intramolecular contacts involving its neighboring residues, Ile243 and Phe245. In PBP5, the analogous Arg248 is flanked by Gly247 and Glu249, which establish few contacts with surrounding residues and allow more conformational freedom for this residue.

Two active site loops, residues 79–83 and 212–218, exhibited flexibility among the four monomers, with some backbone atoms moving by as much as 6 Å from monomer to monomer. These loops also exist in the structure of PBP5 and they interact with the ligand in a structure of PBP5 complexed to a tripeptide boronate transition-state analog.[20] The PBP5 loop corresponding to residues 79–83 maintains nearly identical conformations in all structures of the wild-type PBP5 (determined at 1.6–2.0 Å, comparable to the resolutions of the new PBP6 structures), whether in the presence or absence of ligands,[19,20] in contrast to what is observed with PBP6. In PBP6, the loop appears to be substantially more flexible: in the apo structures for each enzyme, it has crystallographic temperature factors (B-factors) higher than the rest of the protein (with an average of 65 $Å^2$ for the loop residues and 41 $Å^2$ for the whole protein), whereas in PBP5 this loop has temperature factors close to the protein average (~30 $Å^2$). The greater flexibility of the PBP6 loop may derive from differences in the identity of key residues in this region between the two enzymes, with Ala78, Leu79 and Val84 in PBP6 changed to Val, Phe and Leu in PBP5, respectively. The substitution with smaller hydrophobic residues in all three positions of PBP6 decreases both

contacts inside the loop and those with neighboring regions, and may account for the increased flexibility of this loop in PBP6.

Meanwhile, the PBP5 loop corresponding to residues 212–218 in PBP6 also changes conformations between the apo and ligand-complexed PBP5 structures.[19,20] In the PBP5 complex with a ligand, this loop swings closer toward the active site to interact with the transition-state analog, moving by about 2.7 Å for some backbone atoms, compared with the native uncomplexed state. The flexibility of this loop in the PBP6 structure is more pronounced, with substantial changes in the backbone conformation. In the apo structure, the pairwise rmsd ranges from 0.38 to 1.69 Å among the four monomers when aligning only the loop main chain atoms (28 total). The Cα atom of Ala216 moves by 5.9 Å between different loop conformations. For both PBP6 and PBP5, the temperature factors of this loop (47 $Å^2$ for PB6 and 43 $Å^2$ for PBP5) are slightly higher than the protein average.

In PBP6, two conformations of residues 79–83 and one conformation of residues 212–218 have partly resulted from interactions with another monomer either in the same asymmetric unit or related by crystallographic symmetry. Such restraints on the loop conformations might have been one of the reasons why ampicillin did not react with the majority of the four monomers in the asymmetric unit.

Complex with Substrate Fragment

The substrate fragment, NAM-(L-Ala-D-isoGlu-L-Lys-D-Ala-D-Ala), binds to the dimer interface of PBP6 (Figure 4a). Most of the pentapeptide, including the terminal D-Ala-D-Ala, interacts with the active site of monomer 3. Compared with the apo enzyme, the conformations of key catalytic residues, such as Ser40 and Lys43, are unchanged in the complex with the substrate fragment (Figure 4b). The Ser40Oγ atom is in van der Waals contact (3.8 Å) with the carbonyl carbon atom of the penultimate D-Ala in the substrate peptide bond and poised with proper trajectory for the nucleophilic attack (Figure 4a). This configuration is what would be expected for the Michaelis complex. Whereas it is somewhat surprising that the substrate was captured without having reacted with the serine hydroxyl, three aspects of the enzyme and the crystallography reconcile this with the catalytically competent structure that we believe it represents. First, the enzyme turns over the synthetic peptidoglycan with a K_m of 6.5 ± 0.4 mM and a k_{cat} of 0.15 ± 0.01 s^{-1}. These kinetic parameters indicate that the compound is a substrate, one that is slowly turned over. The enzyme has evolved to turn over the polymeric peptidoglycan and this minimalist synthetic substrate still does not have the full features of the native substrate for PBP6. In the crystal, turnover will be slower still, hence the trapping of the substrate in the preacylation state. Second, the structure was determined at pH 4.5, where the presumptive catalytic base, Lys43, is protonated, further slowing the reaction. Third, the substrate was soaked into the crystals over three hours, rather than cocrystallized, increasing our chances of capturing it in its preacylation, Michaelis form.

The synthetic cell wall surrogate hydrogen bonds extensively with the enzyme (Figure 4). The terminal carboxylate of the stem peptide hydrogen bonds with Ser106 and Thr210, in addition to water-mediated interactions with Arg244 and Thr212. The peptide carbonyl oxygen between the last two D-Ala residues is in the oxyanion hole formed by the backbone amide groups of Ser40 and Thr212. The side chain of Asn108 hydrogen bonds with the carbonyl oxygen of the peptide bond between the penultimate D-Ala and L-Lys (Figure 4b). Hydrogen bonds are also formed between the backbone polar groups of protein residues 81–83 and those of the L-Lys on the substrate. Arg194 establishes both a salt bridge and a water-mediated hydrogen bond with the peptide (top of Figure 4a). A limited number of van der Waals contacts are also observed, including those between the Cα and Cβ atoms of Ser82 and the same atoms of L-Lys. Ser82 is located in a position similar to that of Tyr147 in the

R39 DD-peptidase binding cleft for the D-α-aminopimelyl side chain in previous structures, but forms fewer hydrophobic interactions with the ligand compared with Tyr147.[21] The presence of the substrate peptide in the active site of monomer 3 also induced conformational changes in the two active site loops, residues 79–83 and 212–218, compared with their conformations in the apo state of the respective monomer (Figure 4b). These observations suggest that the multiple conformations observed for these two loops in the four apo monomers may be functionally relevant.

Part of the substrate pentapeptide and the NAM monosaccharide to which it is attached extends out into the dimeric partner, monomer 4, with Ser40Oγ in van der Waals contact (3.5 Å) with the methyl group representing the missing NAG. The sugar moiety establishes two hydrogen bonds with the Asn108 side chain and Ser83 backbone amide group. Another hydrogen bond contact is formed between the Ser82 carbonyl oxygen and the amide group of the L-Ala residue, close to the base of the peptide. Arg194 also hydrogen bonds with the peptide. We do not assign direct functional meaning to these dimer spanning interactions, as they would be sterically disallowed by the polymeric cell wall. Whereas the relevance of the dimer interface *in vivo* is uncertain, we do not expect it to substantially influence the protein–ligand interactions essential for catalysis, due to the exclusive and extensive interactions between the substrate fragment and each monomer at the interface. There is a clear division between the two parts of the substrate fragment interacting with each monomer: residues D-isoGlu-L-Lys-D-Ala-D-Ala almost exclusively interact with monomer 3, while the NAM-L-Ala interacts almost exclusively with monomer 4. In the absence of the dimer interface on the membrane surface, the backbone of the NAG-NAM repeats will be ensconced in this region.

Acyl-enzyme Complex with Ampicillin

Small conformational changes were observed for Ser40 and Lys43 in the acyl-enzyme complex with ampicillin, compared with the apo enzyme (Figure 5). The distance between Lys43Nξ and Ser40Oγ is 3.9 Å, too far for a hydrogen bond. The distances between Lys43Nξ and Asn108Oδ1, His147O, Ser106O are 2.9, 3.2 and 3.4 Å respectively. With an acute angle formed by Lys43Ce, Lys43Nξ and each of these three potential hydrogen bond acceptors, any possible hydrogen bond is likely to be less favorable compared with those formed by Lys43 in the apo and Michaelis complex state. Meanwhile, two ordered active site waters have favorable distances (3.0 Å and 3.1 Å) and geometries relative to Lys43Nξ, suggesting hydrogen bonding. Although the relatively weak density of these two water molecules (observed at 1.5 σ in the 2Fo-Fc map) suggests only partial occupancy, their interactions with Lys43 are consistent with the proposed role of this lysine functioning as the general base to deprotonate the catalytic water during the deacylation reaction. Naturally, in this Ampicillininhibited complex, the attack of the catalytic water on the acylenzyme bond is sterically obstructed by the ligand (see Discussion).

Relative to the preacylation complex with the synthetic peptidoglycan surrogate, there are fewer interactions between ampicillin and the protein in the acyl-enzyme complex. As in the case of the substrate complex, the carbonyl oxygen of the acyl bond remains in the oxyanion hole, with two hydrogen bonds to the backbone amide groups. Salt bridges are formed between Arg244 and the C3 carboxylate group, similar to the interactions observed between Arg244 and the sulfate molecules in the apo active sites. The side chain of Thr212 is also involved in a hydrogen bond with the amide group of ampicillin.

Compared with the apo state in the respective monomer, the active site loop of residues 212–218 exhibited a different conformation (Figure 4b). The interaction between the side chain of Thr212 and the ligand also resulted in changes in its rotameric state. Meanwhile, the conformation of residues 79–83 remained largely unchanged. Unlike the substrate

complex, no contacts were observed between this loop and the ligand in the acyl-enzyme complex.

Discussion

These PBP6 structures capture three different stages of the reaction coordinate, including the first structure between a PBP and a peptidoglycan surrogate containing the complete pentapeptide, representing the preacylation complex. Together with previous studies on other DD-carboxypeptidases such as the *E. coli* PBP5 and the *Streptomyces* R61 DD-peptidase, they illuminate the molecular interactions and conformational changes along the entire reaction coordinate of these LMM PBPs. The complex structures also provide new support for how β-lactam compounds inhibit PBPs by mimicking the substrate and blocking the hydrolysis of the acyl-enzyme intermediate.

Substrate Binding by DD-Carboxypeptidases

The PBP6/ muramyl-peptide complex represents the largest cell-wall analog whose structure has been determined bound to a PBP, and it is interesting to consider its implications for cell wall recognition by these enzymes. DD-Carboxypeptidases like PBP6 cleave the terminal D-Ala of the pentapeptide stems of noncross-linked cell wall polymer. Whereas the synthetic NAM-pentapeptide differs from this native substrate by the absence of an extended backbone of NAG-NAM repeats and the exchange of the diaminopimelyl side chain with a lysine, it is nevertheless the closest sample to the true substrate whose structure has been determined to date. In the complex, the substrate is most tightly recognized in the region of the catalytic residues, with the D-Ala amide carbonyl activated by the oxyanion hole of the enzyme and the terminal carboxylate hydrogen bonding extensively with the enzyme. From the catalytic site, the peptide extends toward the bulk solvent. Whereas hydrogen bonding is largely maintained as the substrate extends away from its C-terminus, geometric complementarity between PBP6 and the substrate diminishes progressively as one approached the regions of the protein where the NAG-NAM backbone would bind. By the time the N-terminal amino acid and the NAM itself is reached, the substrate has left the protein monomer in which the catalytic residues reside to interact with a second protein monomer in the asymmetric unit. As indicated earlier, this dimer interface is likely not to exist on the membrane surface and this is the region where the extended NAM-NAM backbone would bind. This suggests that the key recognition elements between PBP6 and the muramyl peptide are concentrated in the C-terminal portion of the stem peptide, as revealed in our structure of the complex. How likely is this conformation to represent that adopted by other PBPs in complex with cell wall peptides?

In the seat of catalysis, the PBP6 complex resembles that of other PBP/substrate analog complexes, including those of PBP5 and that between an inactive R61 DD-peptidase and a substrate fragment.[26] Thus this part of the structure is largely confirmatory. The new information comes further up the peptide chain. Whereas complexes with further fragments of the stem peptide have been determined with the R39 DD-peptidase, which is homologous to PBP6, the PBP6 complex with the muramyl peptide differs from these, partly because the chemical structure of the peptides differ, partly because the structures of the two enzymes differ in this region, and partly because a larger substrate fragment is determined here. In the R39 complexes with a cephalosporin bearing a diaminopimelate side chain, and with a dipeptide bearing this same amino acid, a well-formed hydrophobic binding pocket recognizes the side chain of diaminopimelate.[21] Conversely, in the muramyl penta-peptide complex with PBP6, a lysine occupies the position of the diaminopimelate, and this lysine is largely solvent exposed. We note that whereas muramyl peptides with a Lys in the third position are found in bacterial cell walls, it is the diaminopimelate form that is native to *E. coli* and thus the natural substrate for PBP6. Still, the hydrophobic pocket that

accommodates the diaminopimelate in the R39 structure is simply absent in PBP6, suggesting that this residue is not key for recognition. Conversely, the backbone conformation of this substrate Lys in the PBP6 structure is firmly restricted by hydrogen bonds between the main chain peptide and the protein (Figure 4). Similar interactions were observed in the PBP5 boronic acid analog structure, suggesting that, through the third Lysine position of the step peptide, the main chain conformation of the substrate is conserved and relevant to enzyme recognition.[20] Past this point inferences becomes more speculative, as the extended muramyl peptide is more complete than previously determined, and does not have a crystallographic precedent with which to compare it. Still, we believe that the PBP6/substrate complex reported herein is likely to be the relevant peptidoglycan complex for other PBPs as well, inclusive of the high-molecular mass PBPs that are the critical targets of β-lactam antibiotics. Superimposition of the PBP6/substrate complex onto the structure of the HMM PBP2a, for instance, suggests that the substrate could largely be accommodated by this enzyme, with the only substantial clash arising from the flexible D-isoGlu chain of the substrate colliding with Tyr446 of PBP2a, which may be easily resolvable. After all, all PBPs intimately recognize the C-terminal, cleavable end of the muramyl-peptide, but they may do so with this machinery displaced in space from the sugar polymer, as suggested by the PBP6/muramyl-peptide complex. In this view, in the high-molecular mass PBPs other domains would be responsible for interactions with the larger cell wall not seen in our complex.

Reaction Coordinate of DD-Carboxypeptidases

With the determination of PBP6 preacylation Michaelis complex, there are X-ray crystal structures of almost every intermediate along the reaction pathway of DD-carboxypeptidases, including a boronic acid transition-state analog complex with PBP5 that mimics both the acylation and deacylation high-energy intermediates, a phosphonate transition-state analog and a product complex with R61 DD-peptidase.[20,21,26,35,40] Structures have also been determined for a noncovalent complex between an inactive R61 DD-peptidase and a substrate fragment containing part of the substrate pentapeptide (glycyl-L-α-amino-ε-pimelyl-D-Ala-D-Ala).[26] Together, these structures underscore the important contribution of Lys43 to both acylation and deacylation, and a potential role for Ser83 in stabilizing the leaving group of the acylation reaction.

In the PBP6 complex with the muramyl pentapeptide substrate fragment, the Ser40Oγ atom is 3.8 Å away from the carbonyl carbon of the peptide bond between the two D-alanines that it is going to attack (Figure 4). Lys43 hydrogen bonds with Ser40, consistent with its role as the general base to deprotonate the nucleophilic serine in the acylation step.[18] The leaving group, the backbone nitrogen of the terminal D-Ala, is in close contact with Ser83Oγ (Figure 4). With a distance of 3.8 Å in the preacylation complex, the two atoms are close enough for the formation of a hydrogen bond in the next step, the acylation transition state, to be plausible. Interestingly, in the transition-state analog structure of PBP5, the Oγ atom of the corresponding serine residue is 3.6 Å away from the boronic acid oxygen mimicking the leaving nitrogen group of the substrate.[20] For both PBP5 and PBP6, the presence of the substrate analog or the transition-state analog was able to induce the conformation of this serine that moves its Oγ closer to the substrate, whereas another conformation, with the Oγ atom forming a hydrogen bond with Gln109O, is observed in the apo enzyme and the acyl-enzyme complex (Figure 5). All this suggests that Ser83 may be able to stabilize the leaving group during the acylation reaction, consistent with previous results showing that deleting this serine and surrounding residues abolished the DD-carboxy-peptidase activity of PBP5.[19]

The hydrogen bonds between Lys43 and two water molecules in the acyl-enzyme complex underlie the proposed role of this lysine as the general base for the deacylation reaction (Figure 5).[17] Both waters are approximately 4 Å away from the carbonyl carbon of the acyl-

bond that is attacked in the deacylation step. Although it is unknown whether one of these water molecules represents the catalytic water, it at least suggests that Lys43 is exposed to the solvent in the acyl-enzyme complex and forms different hydrogen bonds compared with the apo enzyme.

The PBP6 structures also reveal residues essential for anchoring the terminal carboxylate group of the substrate peptide, through direct hydrogen bonds or water-mediated interactions. These include Ser106, Thr210, Thr212, Arg194 and Arg244. Although Arg244 has only water-mediated contact with the substrate carboxylate group, its favorable interactions with the C3 carboxylate group of ampicillin in the acyl-enzyme complex and with the sulfate molecules in the apo protein suggest that it may establish direct salt bridges with the substrate during the reaction, particularly on acylation of the active site and the attendant release of the first product, D-Ala. A salt bridge was also observed previously between the Arg244 equivalent in PBP5 and the ligand carboxylate group.[21]

The contribution of protein flexibility to ligand binding and catalysis is suggested by the variation of active site loop conformations along the reaction coordinate and among different monomers in the asymmetric unit. Residues 212–218 exhibit the most substantial changes in different structures. Particularly, Thr212 interacts with the ligand in both PBP6 complexes, assuming different rotameric states and affecting the backbone conformations of the following residues. Residues 79–83 make extensive contact with the substrate peptide. The disordering of this loop in the PBP5 G105D mutant has been tied to the loss of DD-carboxypeptidase activity of this mutant.[19,22]

As a sidebar, it is intriguing that the muramyl pentapeptide substrate, or a close analog of it, has now been observed in four proteins unrelated by sequence or by fold: the endolysin Cpl-1, an alpha+beta fold, the innate human immunity protein peptidoglycan-recognition protein (PGRP), an alpha/beta amidase fold, phage T4 lysozyme a mostly α-helical protein, and the PBP6 structure described here.[17,34,41,42] Given the differences in the fundamental fold, it is unsurprising that very different recognition patterns are implicated in the different complexes. These structures illustrate that not only can a single enzyme recognize chemically diverse, apparently unrelated ligands, which is widely known, but that the very same ligand can be recognized by evolutionarily diverse, unrelated enzymes, which has perhaps been less appreciated. The foregoing discussion is incidentally entirely consistent with the solution NMR structure of the peptidoglycan, which reveals the saccharide backbone as highly defined as a right-handed helix, but in contrast the pentapeptide as highly mobile.[2] The structurally dynamic peptide is well-suited for entrapment by distinct surfaces in different proteins that recognize it.

Inhibition Mechanism of β-Lactam Compounds

Since the seminal studies of Strominger over 40 years ago, it has long been thought that β-lactams are recognized by PBPs based on their mimicry of the acyl-D-Ala-D-Ala portion of the peptidoglycan.[27] The PBP6 complex with the synthetic peptidoglycan surrogate provides a structural context to understand this mimicry. When a noncovalent structure of a complex of R61 DD-peptidase and a β-lactam compound, previously determined by Pratt, Kelly and colleagues, is superimposed onto the PBP6 substrate complex, using only key active site residues, the functional groups of the β-lactam emerge in nearly identical positions compared with those on the peptidoglycan analog (Figure 6).[43] Like the peptidoglycan, the β-lactam ligand places an amide (β-lactam) in the oxyanion hole. The C_3 carboxylate of the β-lactam makes the same hydrogen bonds with Thr210 and Ser106 as does the terminal carboxylate of the substrate stem peptide, and the two groups superimpose almost identically. Similarly, the R1 amide side chain of the β-lactam superimposes with the peptidoglycan, both interacting with Asn108 of PBP6. It is this close correspondence, in the

context of the active site, that allows PBPs to recognize and react with β-lactams, forming an acyl enzyme complex in the same manner as they do with true peptidoglycan substrate.[44,45]

Once the acyl enzyme forms, PBPs become irreversibly inhibited by β-lactams.[44,45] Comparing the acyl-enzyme complex of PBP6/Ampicillin with a boronic acid transition-state analog structure of PBP5 reveals why this is so.[20] When the boronic acid, mimicking the deacylation transition-state species, is superimposed onto the acyl-enzyme complex, it is apparent that the β-lactam-thiazolidine bridging carbon atom of ampicillin lies less than 2 Å away from the boronic acid oxygen that represents the hydrolytic water in the transition state (Figure 7). This steric clash, also observed by others in the structures of related PBPs,[43] would preclude the approach of the hydrolytic water on the acyl-enzyme species for the deacylation half-reaction, preventing the liberation of the enzyme for another catalytic cycle. Conversely, the peptidoglycan substrate, lacking anything analogous to the bridge carbon atom of ampicillin, will not suffer such steric encumbrance and is competent to undergo facile deacylation.

Consistent with the analysis of Strominger 45 years ago, it is the peculiar structure and chemistry of the β-lactam that allows it to mimic the acyl-D-Ala-D-Ala geometry of the peptidoglycan stem peptide, and so be recognized by the enzyme. Combined with earlier studies by Pratt, Knox, Kelly and colleagues, a contribution of the present work is to reveal the structural bases of the mimicry of a β-lactam for a full muramyl peptide substrate, in the active site of a wild-type penicillin-binding protein. Indeed, the structure of the muramyl peptide determined here may be sufficiently complete as to provide a foundation for detailed models of PBP interactions with the full cell wall polymer that is, after all, their native substrate.

Acknowledgments

Supported by NIH grants GM63815 (to B.K.S.) and GM61629 (to S.M.). We thank Hao Fan for helping with homology modeling, and Denise Teotico and Veena Thomas for reading this manuscript.

References

1. Scheffers DJ, Pinho MG. Microbiol. Mol. Biol. Rev. 2005; 69:585–607. [PubMed: 16339737]
2. Meroueh SO, Bencze KZ, Hesek D, Lee M, Fisher JF, Stemmler TL, Mobashery S. Proc. Natl. Acad. Sci. U.S.A. 2006; 103:4404–4409. [PubMed: 16537437]
3. Macheboeuf P, Contreras-Martel C, Job V, Dideberg O, Dessen A. FEMS Microbiol. Rev. 2006; 30:673–691. [PubMed: 16911039]
4. Sauvage E, Kerff F, Terrak M, Ayala JA, Charlier P. FEMS Microbiol. Rev. 2008; 32:234–258. [PubMed: 18266856]
5. Strynadka NC, Adachi H, Jensen SE, Johns K, Sielecki A, Betzel C, Sutoh K, James MN. Nature. 1992; 359:700–705. [PubMed: 1436034]
6. Lim D, Strynadka NC. Nat. Struct. Biol. 2002; 9:870–6. [PubMed: 12389036]
7. Gherman BF, Goldberg SD, Cornish VW, Friesner RA. J. Am. Chem. Soc. 2004; 126:7652–7664. [PubMed: 15198613]
8. Goldberg SD, Iannuccilli W, Nguyen T, Ju J, Cornish VW. Protein Sci. 2003; 12:1633–1645. [PubMed: 12876313]
9. Fisher JF, Meroueh SO, Mobashery S. Chem. Rev. 2005; 105:395–424. [PubMed: 15700950]
10. Kelly JA, Dideberg O, Charlier P, Wery JP, Libert M, Moews PC, Knox JR, Duez C, Fraipont C, Joris B, et al. Science. 1986; 231:1429–1431. [PubMed: 3082007]
11. Knox JR, Moews PC, Frere JM. Chem. Biol. 1996; 3:937–947. [PubMed: 8939710]

12. Nukaga M, Mayama K, Hujer AM, Bonomo RA, Knox JR. J. Mol. Biol. 2003; 328:289–301. [PubMed: 12684014]
13. Ghosh AS, Chowdhury C, Nelson DE. Trends Microbiol. 2008; 16:309–317. [PubMed: 18539032]
14. Tamura T, Imae Y, Strominger JL. J. Biol. Chem. 1976; 251:414–423. [PubMed: 1391]
15. Spratt BG, Strominger JL. J. Bacteriol. 1976; 127:660–663. [PubMed: 776946]
16. van der Linden MP, de Haan L, Dideberg O, Keck W. Biochem. J. 1994; 303:357–362. [PubMed: 7980393]
17. Shi Q, Meroueh SO, Fisher JF, Mobashery S. J. Am. Chem. Soc. 2008; 130:9293–9303. [PubMed: 18576637]
18. Zhang W, Shi Q, Meroueh SO, Vakulenko SB, Mobashery S. Biochemistry. 2007; 46:10113–10121. [PubMed: 17685588]
19. Nicholas RA, Krings S, Tomberg J, Nicola G, Davies C. J. Biol. Chem. 2003; 278:52826–52833. [PubMed: 14555648]
20. Nicola G, Peddi S, Stefanova M, Nicholas RA, Gutheil WG, Davies C. Biochemistry. 2005; 44:8207–8217. [PubMed: 15938610]
21. Sauvage E, Powell AJ, Heilemann J, Josephine HR, Charlier P, Davies C, Pratt RF. J. Mol. Biol. 2008; 381:383–393. [PubMed: 18602645]
22. Davies C, White SW, Nicholas RA. J. Biol. Chem. 2001; 276:616–623. [PubMed: 10967102]
23. de Pedro MA, Young KD, Holtje JV, Schwarz H. J. Bacteriol. 2003; 185:1147–1152. [PubMed: 12562782]
24. Nelson DE, Young KD. J. Bacteriol. 2000; 182:1714–1721. [PubMed: 10692378]
25. Nelson DE, Young KD. J. Bacteriol. 2001; 183:3055–3064. [PubMed: 11325933]
26. McDonough MA, Anderson JW, Silvaggi NR, Pratt RF, Knox JR, Kelly JA. J. Mol. Biol. 2002; 322:111–122. [PubMed: 12215418]
27. Tipper DJ, Strominger JL. Proc. Natl. Acad. Sci. U.S.A. 1965; 54:1133–1141. [PubMed: 5219821]
28. Otwinowski Z, Minor W. Methods Enzymol. 1997; 276:307–326.
29. McCoy AJ, Grosse-Kunstleve RW, Adams PD, Winn MD, Storoni LC, Read RJ. J. Appl. Crystallogr. 2007; 40:658–674. [PubMed: 19461840]
30. Pieper U, Eswar N, Davis FP, Braberg H, Madhusudhan MS, Rossi A, Marti-Renom M, Karchin R, Webb BM, Eramian D, Shen MY, Kelly L, Melo F, Sali A. Nucleic Acids Res. 2006; 34:D291–D295. [PubMed: 16381869]
31. Marti-Renom MA, Stuart AC, Fiser A, Sanchez R, Melo F, Sali A. Annu. Rev. Biophys. Biomol. Struct. 2000; 29:291–325. [PubMed: 10940251]
32. Collaborative Computational Project Number 4. Acta Crystallogr. D: Biol. Crystallogr. 1994; 50:760–763. [PubMed: 15299374]
33. Emsley P, Cowtan K. Acta Crystallogr. D: Biol. Crystallogr. 2004; 60:2126–2132. [PubMed: 15572765]
34. Cho S, Wang Q, Swaminathan CP, Hesek D, Lee M, Boons GJ, Mobashery S, Mariuzza RA. Proc. Natl. Acad. Sci. U.S.A. 2007; 104:8761–8766. [PubMed: 17502600]
35. Kishida H, Unzai S, Roper DI, Lloyd A, Park SY, Tame JR. Biochemistry. 2006; 45:783–792. [PubMed: 16411754]
36. Jelsch C, Mourey L, Masson JM, Samama JP. Proteins. 1993; 16:364–383. [PubMed: 8356032]
37. Chen Y, Delmas J, Sirot J, Shoichet B, Bonnet R. J. Mol. Biol. 2005; 348:349–362. [PubMed: 15811373]
38. Chen Y, Bonnet R, Shoichet BK. J. Am. Chem. Soc. 2007; 129:5378–5380. [PubMed: 17408273]
39. Minasov G, Wang X, Shoichet BK. J. Am. Chem. Soc. 2002; 124:5333–5340. [PubMed: 11996574]
40. Silvaggi NR, Anderson JW, Brinsmade SR, Pratt RF, Kelly JA. Biochemistry. 2003; 42:1199–1208. [PubMed: 12564922]
41. Kuroki R, Weaver L, Matthews BW. Science. 1993; 262:2030–2033. [PubMed: 8266098]

42. Perez-Dorado I, Campillo NE, Monterroso B, Hesek D, Lee M, Paez JA, Garcia P, Martinez-Ripoll M, Garcia JL, Mobashery S, Menendez M, Hermoso JA. J. Biol. Chem. 2007; 282:24990–24999. [PubMed: 17581815]

43. Silvaggi NR, Josephine HR, Kuzin AP, Nagarajan R, Pratt RF, Kelly JA. J. Mol. Biol. 2005; 345:521–533. [PubMed: 15581896]

44. Lee W, McDonough MA, Kotra L, Li ZH, Silvaggi NR, Takeda Y, Kelly JA, Mobashery S. Proc. Natl. Acad. Sci. U.S.A. 2001; 98:1427–1431. [PubMed: 11171967]

45. Lee M, Hesek D, Suvorov M, Lee W, Vakulenko S, Mobashery S. J. Am. Chem. Soc. 2003; 125:16322–16326. [PubMed: 14692773]

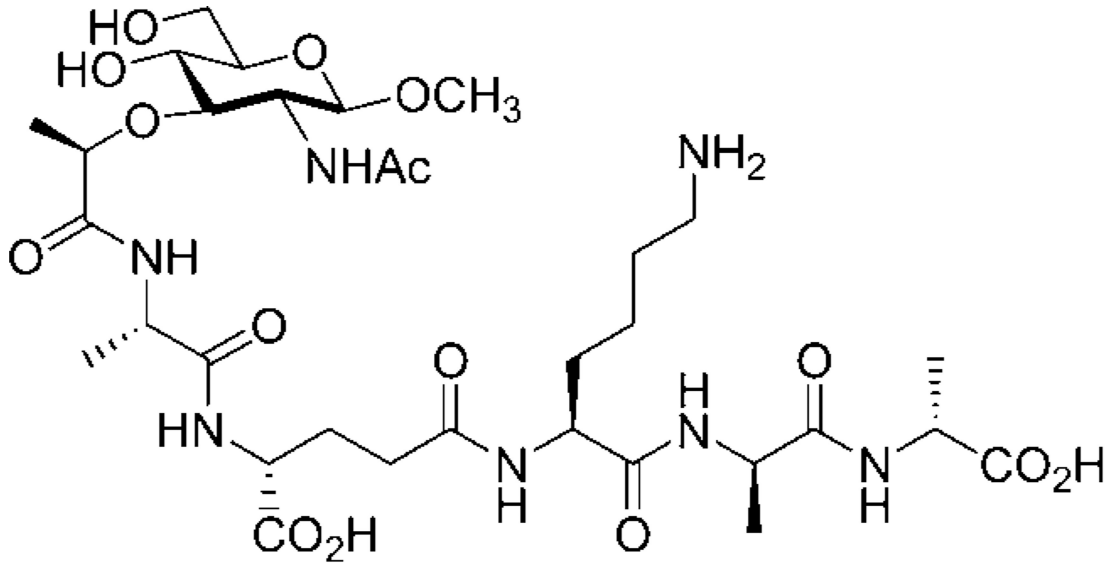

(a)

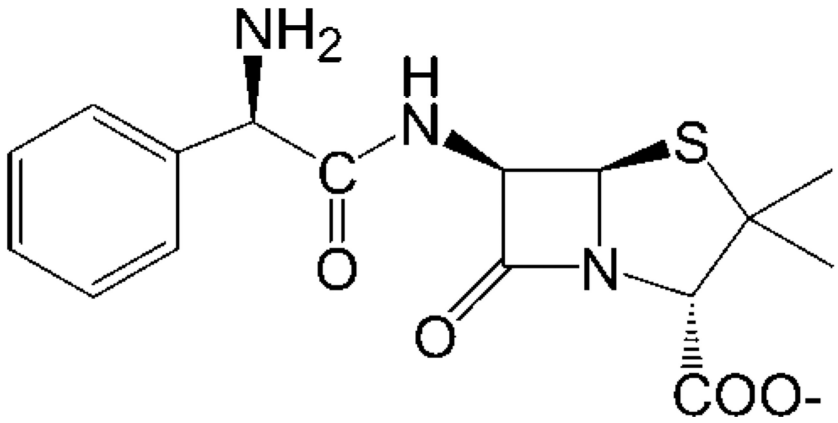

(b)

Figure 1.
Chemical structures of ligands. (a) Synthetic peptidoglycan surrogate, NAM-(L-Ala-D-isoGlu-L-Lys-D-Ala-D-Ala). (b) Ampicillin.

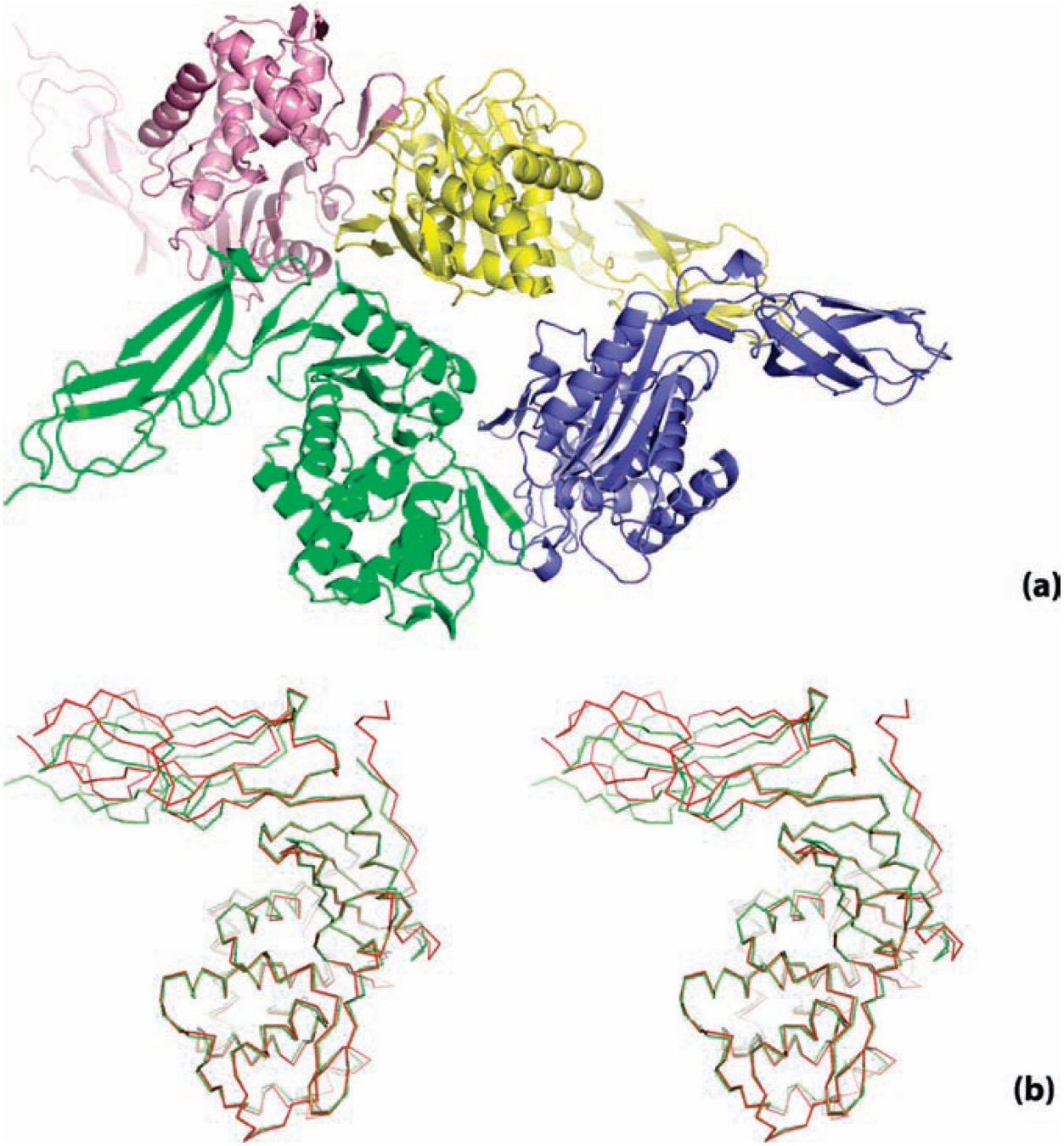

Figure 2.
Overall structure of apo PBP6. (a) Four PBP6 monomers in the asymmetric unit, organized as two similar dimers (green/blue and pink/yellow). (b) Stereo view of the Cα trace of PBP6 (green) superimposed on that of PBP5 (red). Each PBP6 monomer consists of a large N-terminal domain (bottom) and a small C-terminal domain (top).

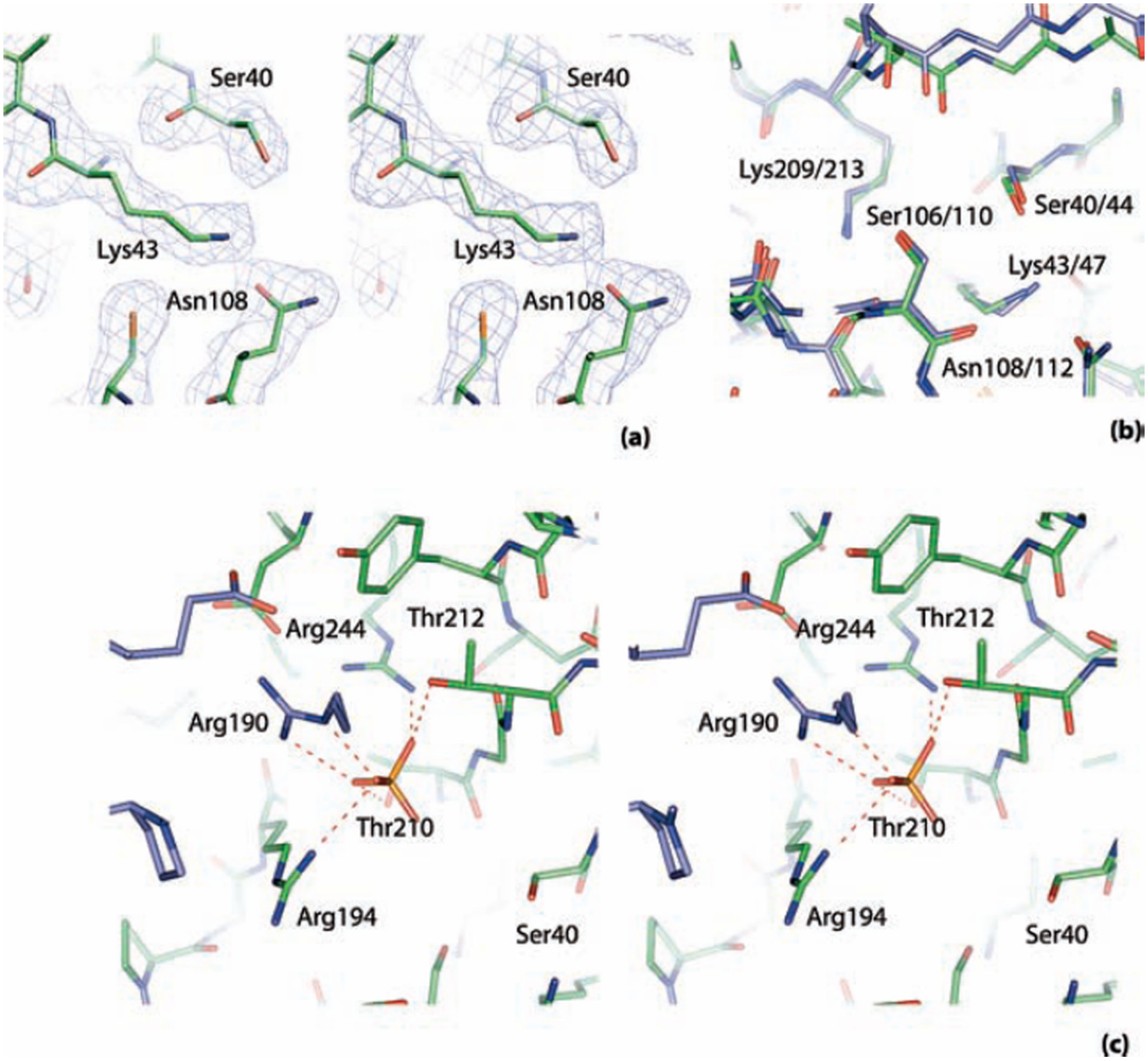

Figure 3.

Active site of apo PBP6. (a) Stereo view of 2Fo-Fc electron density (1.5 σ, in blue) of active site residues. (b) PBP6 (green) active site superimposed on that of PBP5 (blue). (c) Stereo view of residues interacting with the sulfate molecule in the active site of PBP6 monomer 2 (green). The active site resides close to the dimer interface with monomer 1 (blue). The side chain of Arg190 from monomer 1 also interacts with the sulfate molecule.

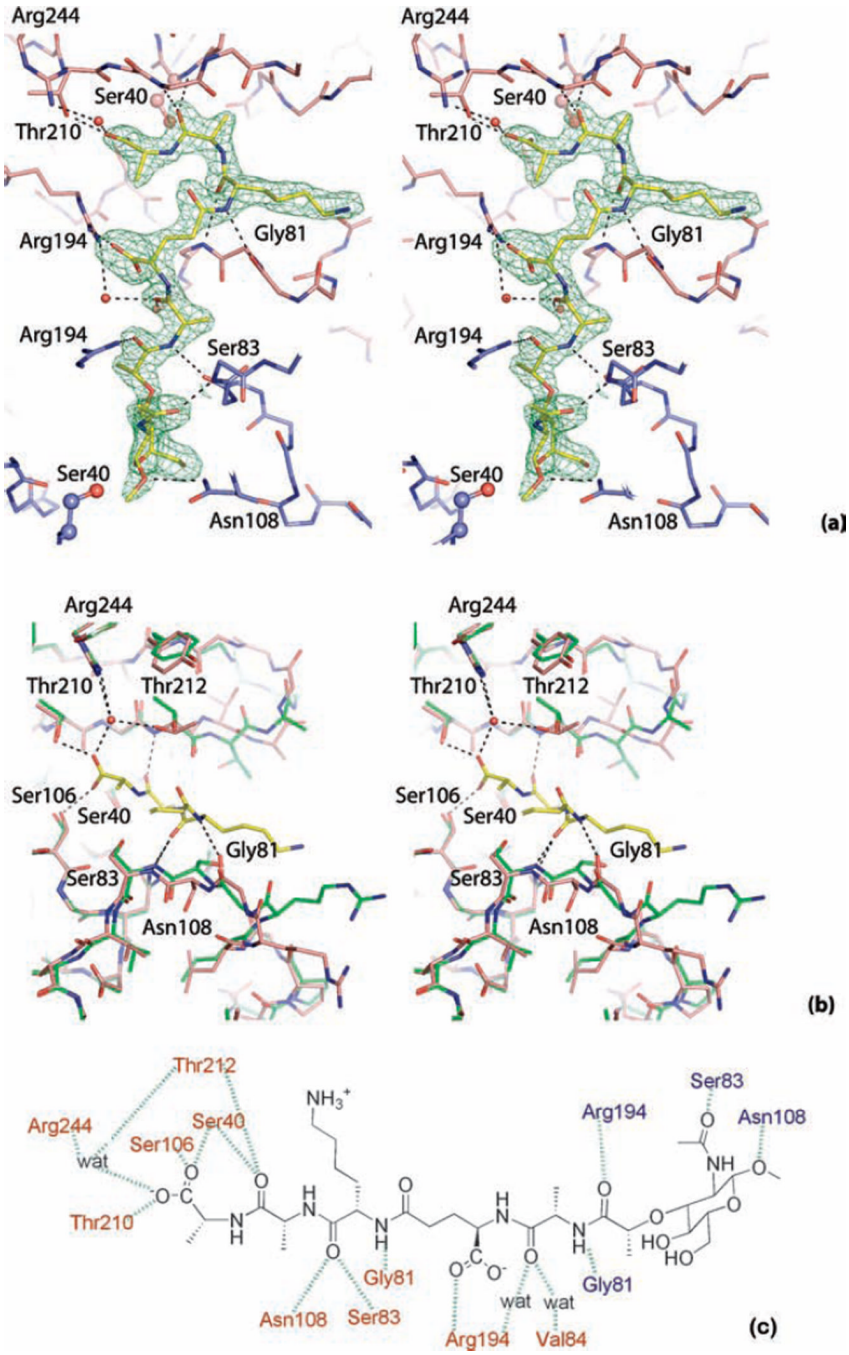

Figure 4.

PBP6 complex structure with the synthetic muramyl-pentapeptide substrate surrogate. (a) Stereo view of the ligand (yellow) at the dimer interface, with 2Fo-Fc density map contoured at 1.5 σ (green). The end of the stem peptide is placed in the active site of monomer 3 (pink) shown at the top, while the sugar moiety is near the active site of monomer 4 (blue). The catalytic serine is shown in ball and stick. Protein side chains not interacting with the ligand are omitted for clarity. Hydrogen bonds are shown as black dashed lines. (b) Stereo view of the complex structure (pink) containing the reaction center, D-Ala-D-Ala of the stem peptide, in comparison to the apo structure of the same monomer (green). (c) Diagram of hydrogen bonding interactions between the substrate fragment and

the side chain or main chain atoms of PBP6 residues. Hydrogen bonds are shown as green dashed lines. Residues from monomer 3 are labeled in red and those from monomer 4 in blue.

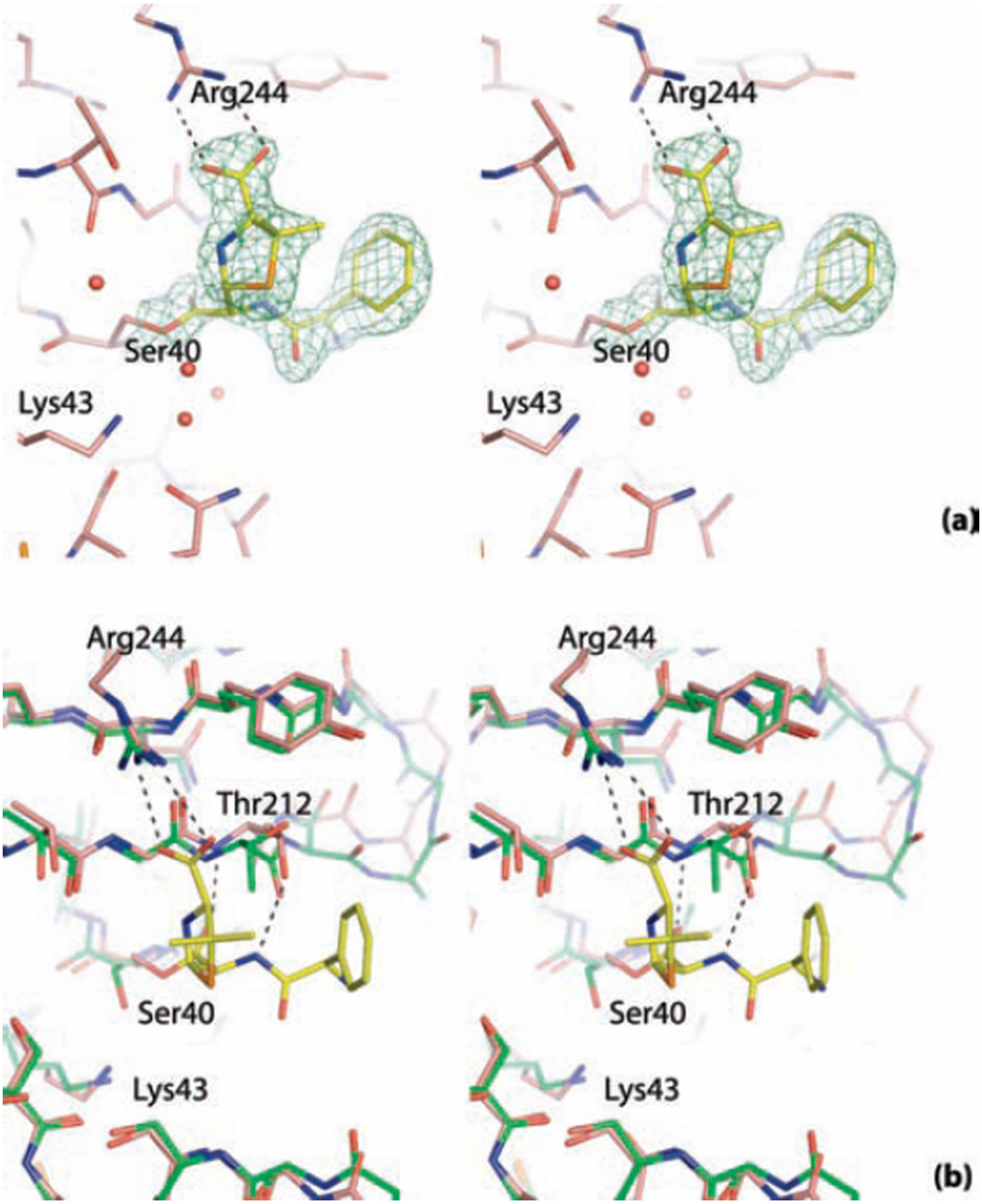

Figure 5.
Structure of the PBP6 acyl-enzyme complex with ampicillin. (a) Stereo view of the ligand (yellow) in monomer 1 (pink), with the 2Fo-Fc density map contoured at 1.5 σ (green). Water molecules are shown as red spheres and hydrogen bonds as black dashed lines. (b) Stereo view of the complex structure (pink) in comparison to the apo structure of the same monomer (green).

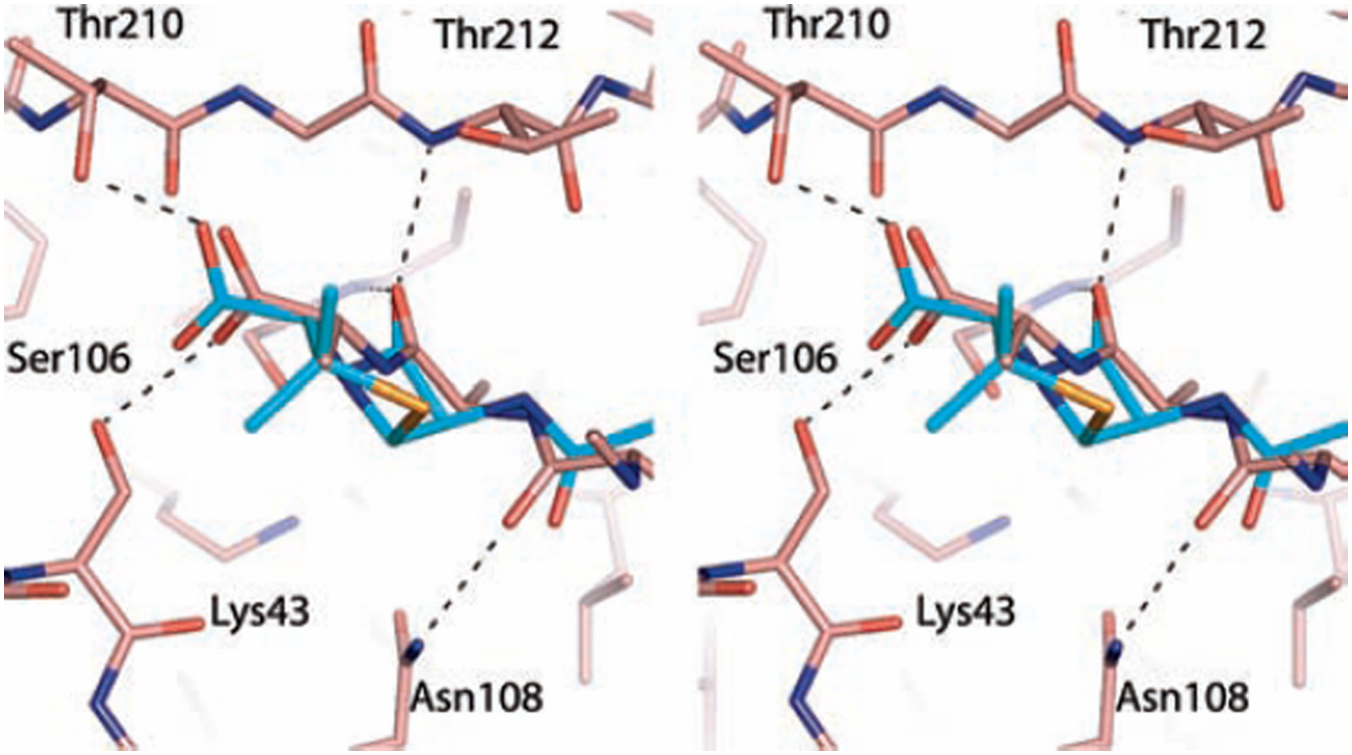

Figure 6.
Similarity between β-lactams and the D-Ala-D-Ala of the substrate, shown in stereo view. The structure of a *nonco Valent* complex between R61 DD-peptidase and aβ-lactam (carbons in blue, PDB 1PW1) is superimposed onto the PBP6 structure with the substrate fragment (carbons in pink), using active site residues 39, 40, 43, 210 and 212.

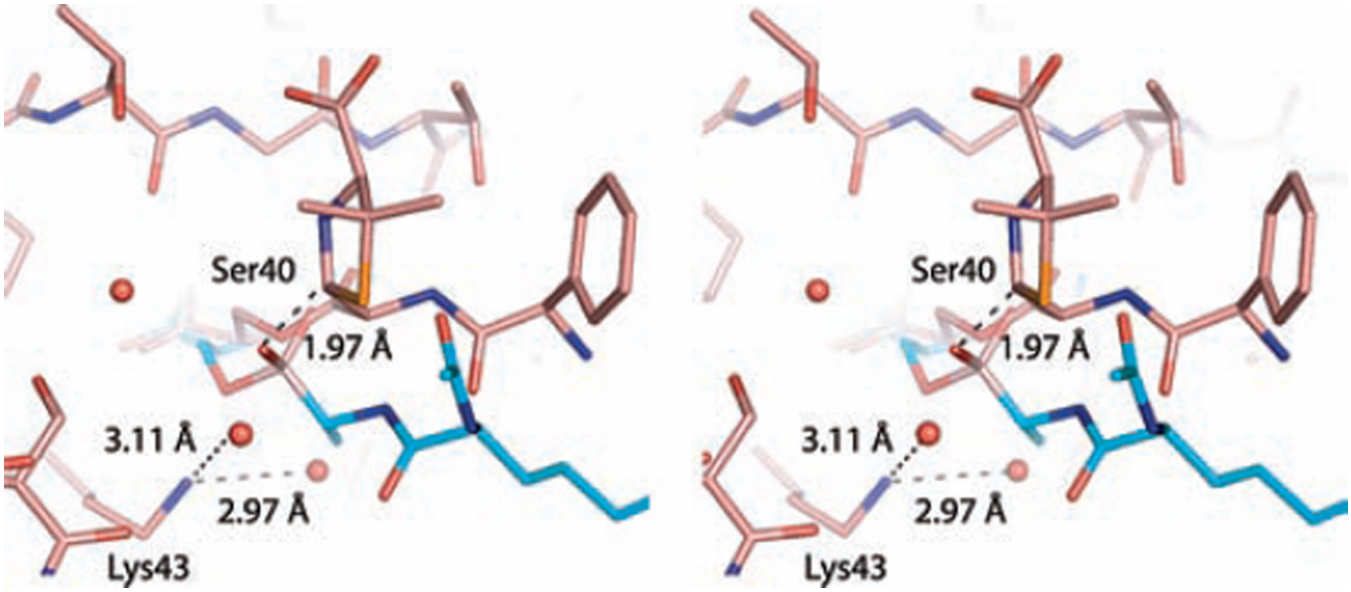

Figure 7.

PBP6 acyl-enzyme complex compared to the deacylation transition state, shown in stereo view. A PBP5 transition-state analog structure (PDB ID, 1Z6F) is superimposed onto the PBP6 structure with ampicillin, using active site residues 39, 40, 43, 108, and 210. The transition-state analog and the catalytic serine of PBP5 are shown in blue, whereas ampicillin and PBP6 are shown in pink. Water molecules represented as red spheres. Key distances are displayed as dashed lines. Lys43 hydrogen bonds with two water molecules in the PBP6 acyl-enzyme complex. The distance is only 1.97 Å between the β-lactam-thiazolidine bridging carbon atom on ampicillin and the boronic acid oxygen of the superimposed transition state analog.

Table 1

Crystallographic Statistics

	Apo	subtrate analog	ampicillin
Data collection			
Space group	$P2_1$		
Cell dimensions			
a, *b*, *c* (Å)	56.949, 184.853, 81.610	57.534, 185.351, 82.329	56.938, 85.980, 83.036
α, β, γ (deg)	90.000, 100.621, 90.000	90.000, 100.993, 90.000	90.000, 101.371, 90.000
Resolution (Å)	50.0–2.10 (2.18–2.10)[a]	50.0–1.80 (1.86–1.80)	50.0–1.80 (1.86–1.80)
R_{merge} (%)[b]	4.2 (36.2)	7.2 (45.9)	2.2 (33.2)
$I/\sigma I$	13.4 (2.0)	13.6 (2.0)	27.1 (2.0)
Completeness (%)	97.7 (97.0)	88.0 (84.0)	95.0 (91.8)
Refinement			
R_{work}/R_{free}	20.7/25.9	20.5/25.4	20.3/25.0
No. atoms			
Protein	10 643	10 669	10 695
Ligand/ion	40	130	49
Water	421	699	774
rms deviations[c]			
bond length (Å)	0.011	0.009	0.011
bond angle (deg)	0.858	1.733	1.322
B factor (Å^2)			
protein	40.8	38.1	38.3
ligand/ion	54.4	47.7	48.3
water	39.7	42.4	41.3

[a] Values in parentheses represent highest resolution shells.

[b] Calculated by Scalepack.[28]

[c] Refined by Refmac in CCP4.[32]